Evaluation of Transient Thermoreflectance of Porous Silicon Membranes for Thermal Interface Applications

Ammar T. Zakar [1]
Hala N. Mohammed [1]
Thoalfiqar A. Zaker [2,3]

[1] *Department of Physics, College of Education for Pure Sciences, University of Mosul, Mosul, IRAQ*
[2] *Department of Physics, College of Education, University of Al-Hamdaniya, Al-Hamdaniya, Mosul, IRAQ*
[3] *Department of Laser and Spectroscopy, Laser and Photonics Research Center, University of Al-Hamdaniya, Al-Hamdaniya, Mosul, IRAQ*

This work involves investigation and separation of the plasmonic and thermal carrier dynamics of porous silicon membrane. The time resolved reflectance and transmittance of the nanoporous membrane were measured using optical pump-MWIR probe approach. The obtained results analyzed using thermal model formulated based on the analytical solution of the Green function. The experimental results were fitted using the model to separate the thermal reflectivity due lattice and plasma reflectivity of the nanoporous. Based on that, the temperature evolution, the thermal dissipation time as well as the thermoreflectance coefficient were extracted.

***Keywords*:** MWIR; Porous silicon; Thermoreflectance; Thermal materials
Received: 03 December 2023; **Revised:** 04 January; **Accepted:** 11 January 2024

1. Introduction

In the recent semiconductor technologies, the knowledge about the optical and thermal properties of semiconductors play a significant role in the wide range of applications such as sustainable energy, energy saving using insulating materials and the heat released from miniaturized electronic devices [1]. It is well-known that the main drawback in the semiconductor devices is the heat generated during device operation. Thus, heat management is crucial to achieve an efficient high power density operation [2,3]. The thermoelectric properties of silicon or silicon derivative materials such as thin or structured silicon films have been extensively studied using different spectroscopic configurations [4-7]. In terms of the device fabrication, the pre-mentioned forms of the silicon require a relatively complex fabrication approaches. Thus, conversion of such silicon forms into real operating devices remain challenging. In contrast, the nanoporous silicon possesses advantages such as abundance and simple fabrication process. The thermal and electrical properties of different porous silicon forms have been widely investigated as a potential candidate in the field of insulating material and optoelectronics devices [8-10]. Some of the silicon forms such as c-Si are commonly used in the fabrication of temperature based sensors. However, the drawback of such forms is the high thermal conductivity (156 W.m/K at room temperature) causing unwanted thermal dispersion when attached to sensing element [11]. Depending on the porosity and the morphology of the porous silicon, lower thermal conductivity of PS can be achieved allowing its use as an alternative candidate of the problem. For the high power electronics (packages or modules), the need for heat dissipative materials with effective dissipation times is crucial to reduce the thermal resistances along the heat conduction path [12-17]. Regarding investigation approaches, many configurations have been utilized to evaluate the thermal properties of different materials such as substrates and thin films [18-20]. Among of which the technique invented in the past decades named noncontact thermoreflectance approach. This investigation method can be used in different configurations including transient thermal imaging, time domain thermoreflectance, transient thermoreflectance (TTR), frequency domain thermoreflectance (FDTR) and many more [21-26]. The availability of femtosecond laser pulses provided the possibility of identifying three regimes of heat transfer during the laser irradiation. The first stage involves laser absorption by electrons and can be classified as nonequilibrium thermal state of the electrons. In the second stage the excited electrons reaches a thermodynamic state so the density of states can be described according to Fermi-Dirac distribution. At this stage, the non-equilibrium thermal state remains dominant and the heat transfer is attributed to the diffusion of hot electrons. Finally, the regime reaches thermal equilibrium condition and most of the energy is transferred to bulk through

electron diffusion [27]. It has been shown that the thermal transport depends mainly on the pulse duration of the laser source. In the case of long pulse durations (nanosecond or longer), the employed model should treat the thermal transport according to Fourier's law while for the short pulses (pico or femto-second pulses) the contribution of the electrons as well as the phonons should be considered [28].

This work provides essential information regarding the dynamics of heat dissipation and reveals the characteristic time that should be taken into account to avoid heat accumulation whenever porous silicon is used in the field of optoelectronic devices.

2. Theoretical Treatment

For a dielectric film, the reflection and transmission of the film is related to the complex refractive index ($N = n + ik$) [29]. Accordingly, any change in the refractive index results in a change in the reflection and transmission of the sample. Thus, for unexcited sample, the reflection of the sample can be expressed as follows:

$$\Delta R = \left(\frac{dR}{dn}\right)_{n_o} \Delta n + \left(\frac{dR}{dk}\right)_{k_o} \Delta k \qquad (1)$$

For the excited sample, the change in the complex refractive index due to temperature can be expressed as follows

$$\Delta N = \left(\frac{dn}{dT}\right) \Delta T + i \left(\frac{dk}{dT}\right) \Delta T \qquad (2)$$

where T represents the temperature. According to the equations above, the change in the reflectivity can be linked with the change in temperature as first order approximation as follows:

$$\Delta R = \left(\frac{dR}{dn}\frac{dn}{dT} + \frac{dR}{dk}\frac{dk}{dT}\right) \Delta T = F(n_o)\Delta T \qquad (3)$$

The transient thermal profile of the solid slab excited by pulsed laser can be mathematically treated based on the instantaneous heat source or so called Green function approach [30]. This technique involves of using the solution $F(r, r', t = 0) = \delta(r - r')$ as a Green function acting at time (t=0) for the differential equation as follows:

$$\left(\nabla_r^2 - \frac{1}{\alpha}\frac{d}{dt}\right) F(r, r', t) = 0 \qquad (4)$$

where α refers to the thermal diffusivity. The physical interpretation of such function can be understood as a temperature rise due to the instantaneous heat source acting on the point r at time t=0. By substituting the green function describing this process and Integrating the resulted formula based on the spatial variables (x',y',z'), the induced temperature due to instantaneous and extended heat source can be obtained. This also provides the possibility of solving the heat equation in specific cases where the regular geometry of the heating source and temperature distribution of the heated sample are given at t=0. In the case of laser irradiated membrane, the heating rises instantly along the z axis of the laser. Thus, in terms of heat conduction, the z-coordinate becomes irrelevant in practice and the sample can be mathematically treated in two spatial dimensions. Here, the pumping beam is approximated to be cylindrical with radius a on the sample plane. In order to obtain an analytical solution, some approximations should be considered. First, the drop of the field energy – density should be neglected along the propagation path. Second, the initial temperature of the membrane induced by the pumping laser should be approximated with a step function which can be employed as initial condition in the rest of the solution processes. This yields an analytical solution expressed as follows:

$$T = (r = 0, t) = T_o \left(1 - e^{\left(\frac{-a^2}{4\alpha t}\right)}\right) \qquad (5)$$

The above solution is valid only if the axis r=0 is considered. Moreover, the decay approximation is valid if the spot size of the probe signal is smaller than that of the pump. The decay term can be utilized to estimate the decay of the probe signal at t>0. Here, t represents the delay time between the pump and probe signals. By fitting the probe signal using the equation above, the heat dissipation time ($\tau = \frac{a^2}{4\alpha}$) and hence the thermoreflecatnce coefficient can be extracted. More information about the solution processes can be found elsewhere [30].

3. Sample and Setup

The sample in this study was fabricated based on electro-chemical anodization of Si (100) wafer. The etching process was done by the combination of methanol electrolyte and 40% of HF with ratio of 1:1 at 30 mA/cm^2 current density. The porous layer then separated from the underlying substrate using a current pulse of about 120 mA/cm^2 for 10 s. The thickness of the nanoporous sample was 27 µm containing silicon fibrils with average diameter about 10 nm as shown in the Fig. (1).

The coherent laser system was used to measure the transient reflectance and transmittance of the sample based on pump-probe technique. The emerging power was around 3.2 W at 800 nm wavelength and 1 kHz reputation rate. The pulse duration at FWHM was around 60 fs measured using autocorrelation. The emerging beam then separated into two components with average power of about 0.12 and 3 W respectively. The later beam was guided into the optical parametric amplifier (OPA) to generate probe beam in the MWIR range while the weaker is used as pumping source. The tunable parametric amplifier provides the possibility of generating MWIR wavelengths covering the range from 3.2 to 6 µm. The time delay controlling was achieved using retroreflector mounted on the computerized rotational stage. The output power of the laser was controlled using a combination of polarizer and half wave plate. The pump and probe incident angels with respect to the normal were 60° and 24°, respectively. The polarization of the pump and probe beams was oriented perpendicular to each other to avoid any possible interference. The diameter of the pump and probe beams were 620 and 200 µm,

respectively. The transient reflection was detected using InSb photoconductive detectors.

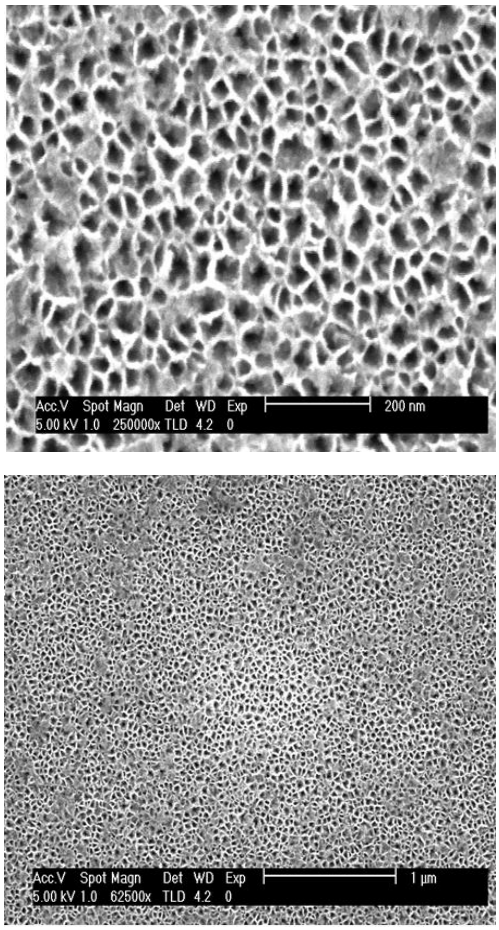

Fig. (1) SEM images of porous silicon membrane. The image on the left represents the zoomed SEM image of the sample

4. Results and Discussion

It is known that the sample exposure to the ultrafast laser causes localized temperature change. The effect of the thermal change can be observed in the transient reflectivity of the sample. It is important to note here that the complex refractive index is influenced by both lattice temperature as well as the rate of generated carriers in the case of semiconductor samples. Thus, the total thermal change should accounts for lattice and plasma contributions respectively [31].

Figure (2) shows the time resolved reflectance and transmittance for 27 µm porous silicon membrane measured at 25 mW pumping power and 4 µm probe wavelength. It can be seen from the figure that the reflectance and transmittance follow the well-known trend of the porous silicon where the probe signal is initially absorbed by the generated carriers at time delay t=0 followed by a decay.

It should be mentioned here that the reflectance and transmittance change encompasses both carrier decay (relaxation and recombination) as well as the contribution of the heat dissipation into the sample structure as shown in the Fig. (2). It has been shown that the recombination time (t_{rec}) of the excited carriers is a fast process ends within 100-200 ps [32]. Thus, the reflectance change is proportional to the temperature only for delay times $t > t_{rec}$.

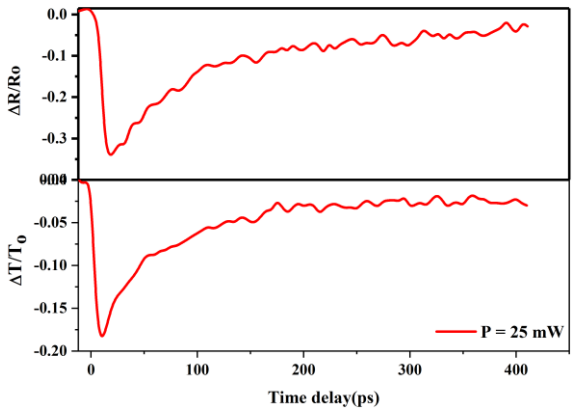

Fig. (2) Time-resolved reflectance and transmittance change of 27µm porous silicon membrane at 25mW pumping power and 4µm probe wavelength

The final analytical expression (Eq. 5) can be used to fit the normalized reflectance shown in the Fig. (3). This can be done by setting the thermal dissipation time as a fitting parameter. The fitting yielded a thermal dissipation time of 95 ps. Using the extracted thermal time, the thermoreflectance data can be recovered as shown in Fig. (4).

As the total thermal effect encompasses both plasma and lattice contributions, the reflectance change caused by plasma contribution can be calculated by simply subtracting the total reflectance change from lattice reflectance as shown in the Fig. (5).

To calculate the temperature evolution of the sample, the thermoreflecatce coefficient should be measured. In fact, this coefficient differs from sample to sample depending on the material and the surface. This in turn depends on many parameters such as wavelength, surface properties, temperature, and material processing in some specific cases. In the case of semiconductors and metals, the value of the thermo-reflectance coefficient is shown to be in the range of 10^{-2}-10^{-5} K^{-1} [33-35]. This coefficient can be measured directly depending on the experiment condition either by measuring the reflectance at different temperature or by combination of Eq. (7) and the well-known reflectance equation $\frac{\Delta R}{R} = k\,\Delta T$ as shown in the Fig. (6), where k represents thermoreflectance coefficient. The extracted thermoreflectance coefficient was found to be around $6.9\text{x}10^{-3}$ K^{-1}.

Based on the obtained thermo-reflectance coefficient, it is possible now to calculate the temperature evolution of the sample by dividing the total reflectance change on the extracted coefficient as shown in Fig. (7).

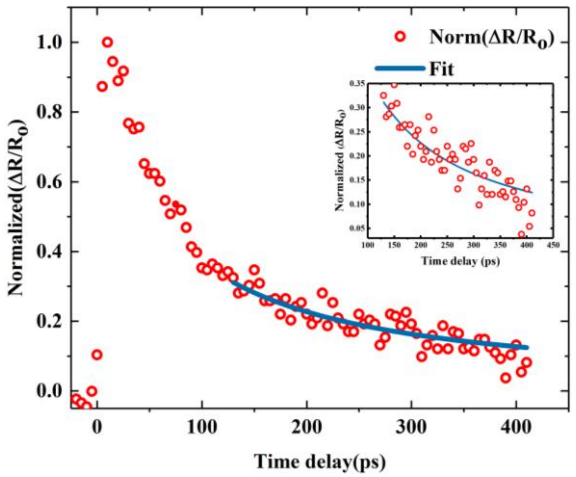

Fig. (3) The normalized reflectance change fitted for $t>t_{rec}$ using Eq. (5). The inset indicates the zoomed fitting range

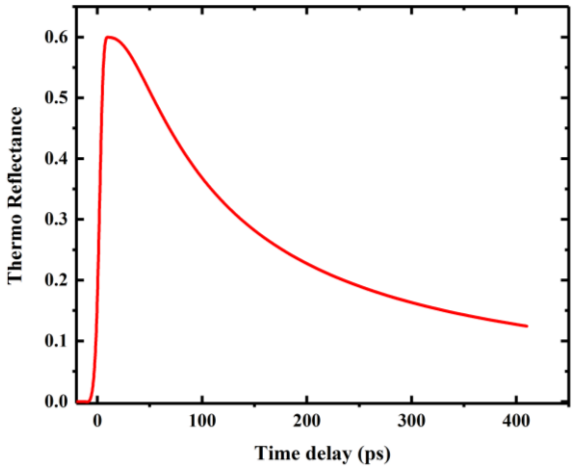

Fig. (4) Thermoreflecatnce data recovered using the analytical solution. The thermal dissipation time is extracted by fitting the analytical solution to the normalized reflectance

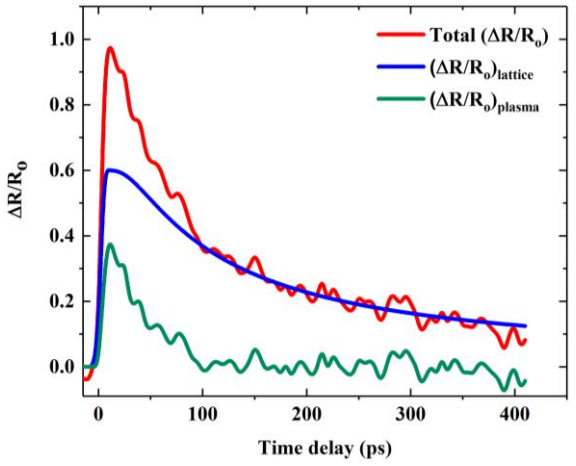

Fig. (5) The total reflectance change (red line), thermoreflectance due to lattice temperature (blue line) as well as the reflectance due to plasma contribution (green line)

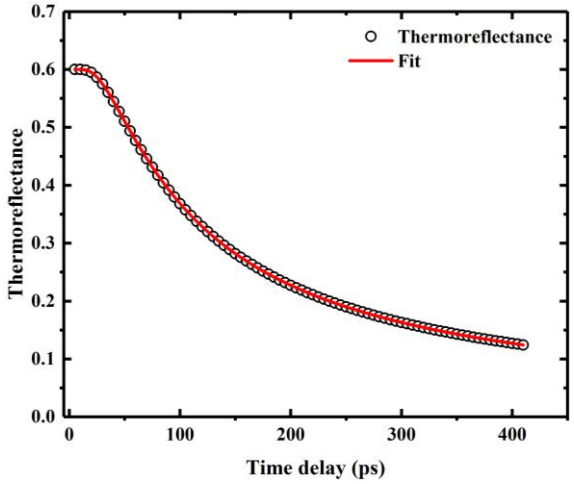

Fig. (6) The thermo-reflectance change fitted using the combination of equation (7) and the reflectance expression $\frac{\Delta R}{R} = k\,\Delta T$. The obtained thermal dissipation time is used to fit the data while k was set as fitting parameter

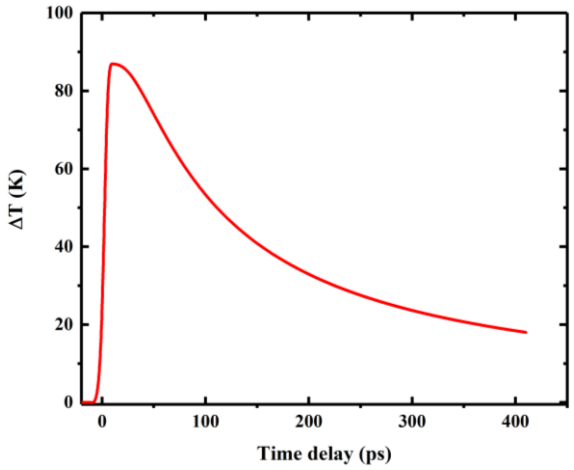

Fig. (7) The temperature evolution of the porous silicon membrane. The temperature of the sample increases at time delay t=0 between pump and probe signals followed by thermal diffusion to the bulk

5. Conclusion

In this work, the time resolved optical pump-MWIR probe was employed to measure the time resolved reflectance and transmittance of the porous silicon membrane with 27µm thickness and porosity of about 63%. To estimate the thermal dissipation time of the sample, the analytical solution based on the Green's function is used to fit the reflected signal data at $t>t_r$ where t and t_r refer to the time delay between the pump and probe signals and the recombination time of the excited carriers respectively. The thermal dissipation time of the sample was found to be 95ps. The estimated time then employed to recover the reflectivity due to lattice temperature. The plasma reflectivity was calculated by simply subtracting the total reflectivity from that of the lattice. The thermoreflectance coefficient of $6.9\text{x}10^{-3}$ K^{-1} is obtained by the combination of the analytical solution and the well known $\frac{\Delta R}{R} = k\,\Delta T$.

Based on the obtained coefficient, the temperature evolution of the porous silicon sample is also calculated. The thermal dissipation time extracted using the analytical model is straightforward comparing to nonlinear models consisting a set of complex equations where the dissipation time turns out to be model dependent parameter.

References

[1] D. Kendig et al., "Accurate thermoreflectance imaging of nano-features using thermal decay", in *2017 16th IEEE Intersoc. Conf. on Therm. Thermomech. Phenom. in Electron. Syst. (ITherm)*, IEEE (20170, pp. 23-29.
[2] M. Kuball et al., "Measurement of temperature in active high-power AlGaN/GaN HFETs using Raman spectroscopy", *IEEE Electron Dev. Lett.*, 23(1) (2002) 7-9.
[3] J. Jeong et al., "Picosecond transient thermoreflectance for thermal conductivity characterization", *Nanoscale Microscale Thermophys. Eng.*, 23(3) (2019) 211-221.
[4] J. De Boor et al., "Thermoelectric properties of porous silicon", *Appl. Phys. A*, 107 (2012) 789-794.
[5] K. Hippalgaonkar et al., "Fabrication of microdevices with integrated nanowires for investigating low-dimensional phonon transport", *Nano Lett.*, 10(11) (2010) 4341-4348.
[6] J. De Boor et al., "Sub-100 nm silicon nanowires by laser interference lithography and metal-assisted etching", *Nanotechnol.*, 21(9) (2010) 095302.
[7] J. Tang et al., "Holey silicon as an efficient thermoelectric material", *Nano Lett.*, 10(10) (2010) 4279-4283.
[8] R.G. Mathur, R.M. Mehra and P.C. Mathur, "Thermoelectric power in porous silicon", *J. Appl. Phys.*, 83(11) (1998) 5855-5857.
[9] G. Gesele et al., "Temperature-dependent thermal conductivity of porous silicon", *J. Phys. D: Appl. Phys.*, 30(21) (1997) 2911.
[10] H. Föll et al., "Formation and application of porous silicon", *Mater. Sci. Eng. R: Rep.*, 39(4) (2002) 93-141.
[11] Y. Ezzahri et al., "Determination of thermophysical properties of Si/SiGe superlattices with a pump-probe technique", In *THERMINIC 2005*, pp. 235-243. TIMA Editions, 2005.
[12] D.D.L. Chung, "Thermal interface materials", *J. Mater. Eng. Perform.*, 10 (2001) 56-59.
[13] J. Due and A.J. Robinson, "Reliability of thermal interface materials: A review", *Appl. Therm. Eng.*, 50(1) (2013) 455-463.
[14] J.P. Gwinn and R.L. Webb, "Performance and testing of thermal interface materials", *Microelectron. J.*, 34(3) (2003) 215-222.
[15] A.J. McNamara, Y. Joshi and Z.M. Zhang, "Characterization of nanostructured thermal interface materials-A review", in *TMNN-2011. Proc. Int. Symp. on Therm. Mater. Nanosci. Nanotechnol.*, Begel House Inc. (2011).
[16] K.C. Otiaba et al., "Thermal interface materials for automotive electronic control unit: Trends, technology and R&D challenges", *Microelectron. Reliab.*, 51(12) (2011) 2031-2043.
[17] R. Prasher, "Thermal interface materials: historical perspective, status, and future directions", *Proc. IEEE*, 94(8) (2006) 1571-1586.
[18] V. Lysenko et al., "Nanoscale nature and low thermal conductivity of porous silicon layers", *Appl. Surf. Sci.*, 123 (1998) 458-461.
[19] G. Kaltsas and A.G. Nassiopoulou, "Novel C-MOS compatible monolithic silicon gas flow sensor with porous silicon thermal isolation", *Sens. Actuat. A: Phys.*, 76(1-3) (1999) 133-138.
[20] M. Boutchich et al., "Characterization of phosphorus and boron heavily doped LPCVD polysilicon films in the temperature range 293-373K", *IEEE Electron Dev. Lett.*, 23(3) (2002) 139-141.
[21] J. Jeong et al., "Picosecond transient thermoreflectance for thermal conductivity characterization", *Nanoscale Microscale Thermophys. Eng.*, 23(3) (2019) 211-221.
[22] A.J. Schmidt, R. Cheaito and M. Chiesa, "A frequency-domain thermoreflectance method for the characterization of thermal properties", *Rev. Sci. Instrum.*, 80(9) (2009) ??-??.
[23] A.J. Schmidt, R. Cheaito and M. Chiesa, "Characterization of thin metal films via frequency-domain thermoreflectance", *J. Appl. Phys.*, 107(2) (2010) ??-??.
[24] K.T. Regner et al., "Broadband phonon mean free path contributions to thermal conductivity measured using frequency domain thermoreflectance", *Nat. Commun.*, 4(1) (2013) 1640.
[25] R. Garrelts, A. Marconnet and X. Xu, "Assessment of thermal properties via nanosecond thermoreflectance method", *Nanoscale Microscale Thermophys. Eng.*, 19(4) (2015) 245-257.
[26] J. Jeong et al., "In-plane thermal conductivity measurement with nanosecond grating imaging technique", *Nanoscale Microscale Thermophys. Eng.*, 22(2) (2018) 83-96.
[27] I.H. Chowdhury and X. Xu, "Heat transfer in femtosecond laser processing of metal", *Num. Heat Transfer A: Appl.*, 44(3) (2003) 219-232.
[28] D. Sands, "Pulsed laser heating and melting", in **"Heat Transfer - Engineering Applications"**, V. Vikhrenko (editor), IntechOpen (2011), Ch. 3, 47-70.
[29] A.G. Cullis, L.T.P.D.J. Canham and P.D.J. Calcott, "The structural and luminescence properties of porous silicon", *J. Appl. Phys.*, 82(3) (1997) 909-965.
[30] U. Bernini et al., "Evaluation of the thermal conductivity of porous silicon layers by an optical pump-probe method", *J. Phys.: Cond. Matter*, 13(5) (2001) 1141.

[31] J. Opsal et al., "Temporal behavior of modulated optical reflectance in silicon", *J. Appl. Phys.*, 61(1) (1987) 240-248.
[32] S.J. Park et al., "All-optical modulation in Mid-Wavelength Infrared using porous Si membranes", *Sci. Rep.*, 6(1) (2016) 30211.
[33] C.V. Cardenas, "Thermoreflectance temperature measurement and application to gold thin films and carbon nanofibers", MSc thesis, Santa Clara University (USA, 2011).
[34] P-L. Komarov, M.G. Burzo and P-E. Raad, "CCD thermoreflectance thermography system: methodology and experimental validation", *arXiv preprint arXiv: 0709.1854* (2007).
[35] C. Cardenas et al., "Thermoreflectance measurement of temperature and thermal resistance of thin film gold", ?? (2012) 111401, pp 2-4.

